Published OnlineFirst December 8, 2009; DOI: 10.1158/0008-5472.CAN-09-2970

Cancer Research

Antigen Presentation by Dendritic Cells in Tumors Is Disrupted by Altered Metabolism that Involves Pyruvate Kinase M2 and Its Interaction with SOCS3

Zhuohan Zhang, Qiaofei Liu, Yongzhe Che, et al.

Cancer Res 2010;70:89-98. Published OnlineFirst December 8, 2009.

Published OnlineFirst December 8, 2009; DOI: 10.1158/0008-5472.CAN-09-2970

Microenvironment and Immunology

Cancer Research

Antigen Presentation by Dendritic Cells in Tumors Is Disrupted by Altered Metabolism that Involves Pyruvate Kinase M2 and Its Interaction with SOCS3

Zhuohan Zhang[1], Qiaofei Liu[1], Yongzhe Che[2], Xin Yuan[1], Lingyun Dai[1], Bin Zeng[1], Guohui Jiao[1], Yin Zhang[1], Xue Wu[1], Yinyan Yu[1], Yuan Zhang[1], and Rongcun Yang[1,3]

Abstract

Dendritic cell (DC) function is negatively affected by tumors and tumor-derived factors, but little is known about the underlying mechanisms. Here, we show that intracellular SOCS3 in DCs binds to pyruvate kinase type M2 (M2-PK), which plays a critical role in ATP production through glycolysis. The interaction of SOCS3 with M2-PK reduced ATP production and impaired DC-based immunotherapy against tumors. Thus, SOCS3, which has been shown to be upregulated by tumor-derived factors, interacts with M2-PK to decrease ATP production, causing DC dysfunction. These dysfunctional DCs have a reduced ability to present antigens. Alteration of DC metabolism mediated by SOCS3 represents a novel mechanism for DC dysfunction in the tumor microenvironment. *Cancer Res; 70(1); 89–98. ©2010 AACR.*

Introduction

Dendritic cells (DC) play a key role in the induction of tumor-specific immune responses, especially by cross-priming, which allows the transfer of antigens from tumor cells to DCs (1, 2). However, DCs in tumor environments often seem to be phenotypically and functionally defective, as reviewed by Gottfried and colleagues (3) and Bennaceur and colleagues (4). Indeed, tumor-associated factors, including cytokines transforming growth factor-β, granulocyte macrophage colony-stimulating factor (CSF), interleukin (IL)-6, macrophage CSF, and IL-10, as well as vascular endothelial growth factor, gangliosides, prostaglandin E_2, and some metabolic products, may affect the function and differentiation of DCs (4). Additionally, hypoxia, low nutrient levels, low extracellular pH, and high interstitial fluid pressure have also emerged as important components contributing to DC dysfunction (5). There is evidence showing that hypoxia can reduce the migratory capacity of human monocyte-derived DCs (6). Experimental hypoxia also alters the morphologic characteristics, expression of cell surface markers, viability, phagocytosis, metabolic activity, and release of cytokines by macrophages (7). Despite the wealth of information about factors that affect the differentiation and function of DCs, little is known about the molecular mechanism(s) responsible for DC dysfunction in cancer.

Suppressor of cytokine signaling 3 (SOCS3), which belongs to the SOCS family of proteins, can be induced and upregulated by not only cytokines such as IL-6 and lipopolysaccharide (LPS) but also tumor-associated factors in DCs (8). SOCS3 contains an NH_2-terminal region (12 residues of a kinase inhibitory region), a central SH2 domain, and a COOH-terminal motif called the SOCS box (9, 10). SOCS3 may use its SH2 domain to bind to phosphorylated tyrosine residues in its partners such as gp130 (Y759), leptinR (Y985), and EpoR (Y401; ref. 11) to regulate their activity. Herein, we found that SOCS3 can directly interact with the pyruvate kinase type M2 (M2-PK), a key enzyme in metabolic pathway of glycolysis, thereby suppressing M2-PK activity. Because SOCS3 can be induced by a wide variety of cytokines (12–14), especially tumor-associated factors (8), the upregulation of SOCS3 in DCs may play an important role in the path toward DC dysfunction, thus causing tumor immune tolerance.

Materials and Methods

Mice. Male C57BL/6 and BALB/c mice, 4 to 6 wk old (Beijing Experimental Animal Center), were maintained in a pathogen-free animal facility for at least 1 wk before use. Experiments were performed in accordance with institutional guidelines.

DCs, cell lines, and antibodies. Mouse bone marrow–derived DCs (BMDC) were prepared as previously described (15). Monocyte/macrophage cell line RAW264.7, murine Lewis lung carcinoma (LLC) cell line, and B16 melanoma cell line were purchased from the American Type Culture Collection. The spontaneously transformed mouse ovarian surface epithelial cell line 1D8 was a gift of Dr. Roby (University of Kansas Medical Center, Kansas City, KS; ref. 16). All of the

Authors' Affiliations: Departments of [1]Immunology and [2]Anatomy, Nankai University School of Medicine and [3]Key Laboratory of Bioactive Materials, Ministry of Education, Nankai University, Tianjin, People's Republic of China

Note: Supplementary data for this article are available at Cancer Research Online (http://cancerres.aacrjournals.org/).

Corresponding Author: Rongcun Yang, Department of Immunology, Nankai University School of Medicine, Nankai University, Tianjin 300071, People's Republic of China. Phone: 86-22-23509007; Fax: 86-22-23502554; E-mail: ryang@nankai.edu.cn.

doi: 10.1158/0008-5472.CAN-09-2970

Published OnlineFirst December 8, 2009; DOI: 10.1158/0008-5472.CAN-09-2970

cell lines were grown in RPMI 1640 supplemented with 10% fetal bovine serum and 1% penicillin/streptomycin.

Phycoerythrin (PE)–labeled or FITC-labeled anti-mouse CD11c (N418), CD80 (16-10A1), CD4 (L3T4), and CD8α (Ly-2) antibodies were purchased from Pharmingen. Rabbit anti-mouse SOCS3 antibodies (Transduction-Becton Dickinson), rabbit anti-mouse M2-PK antibodies (Abcam), goat anti-SOCS3 antibodies (Santa Cruz Biotechnology), PE-labeled donkey polyclonal antibodies against the rabbit IgG-H&L-F(ab)$_2$ fragment (Abcam), FITC-labeled rabbit anti-goat IgG antibodies (Santa Cruz Biotechnology), horseradish peroxidase–labeled goat polyclonal antibodies against rabbit IgG-H&L (Abcam), and FITC-labeled anti-V5 antibodies (Invitrogen) were also purchased.

Immunoprecipitation. For immunoprecipitation, V5-tagged SOCS3 vector–transfected or control plasmid vector–transfected cells were extracted in hypotonic lysis buffer as previously described (8). The nuclei were removed by centrifugation, and then the lysates were precleared with protein G-Sepharose and isotype control antibody. Immunoprecipitation was performed with the anti-V5 antibody and protein G-Sepharose with slow agitation. The immunoprecipitates were washed and resolved by 10% SDS-PAGE and then analyzed by Western blotting. The membranes were developed using the enhanced chemiluminescence (ECL) detection system (Amersham Biosciences).

Matrix-assisted laser desorption/ionization–time-of-flight mass spectrometry and time-of-flight tandem mass spectrometry. For matrix-assisted laser desorption/ionization–time-of-flight mass spectrometry (MALDI-TOF-MS), protein bands from the immunoprecipitation were cut out from the SDS-PAGE gel and washed for 30 min in 100 μL of 50 mmol/L NH_4HCO_3 followed by 100 μL of 50% CH_3CN/50 mmol/L NH_4HCO_3. After evaporating the solution, 100 μL acetonitrile was used to shrink the gel piece for 10 min. The gel piece was reswollen with 0.2 μg trypsin in 20 μL of 25 mmol/L NH_4HCO_3 for 10 min and then covered with 20 μL of 25 mmol/L NH_4HCO_3. Digestion was performed overnight at 37°C. Tryptic peptides were dissolved in 0.5% trifluoroacetic acid and then desalted using ZipTipC18 (Millipore). All mass spectra using MALDI-TOF-MS were done by the Department of Biochemistry, Peking University of Medical School, and obtained on an Ultraflex MALDI-TOF/TOF (Bruker-Franzen) in positive ion mode with an accelerating voltage of 20 kV using α-cyano-4-hydroxycinnamic acid as the matrix. The spectra were internally calibrated using trypsin autolysis products. The obtained peptide mass fingerprints (PMF) were used to search the NCBInr database. TOF-MS/MS of selected polypeptides was performed when PMFs obtained from a particular band did not provide sufficient information for protein identification.

Glutathione S-transferase–SOCS3-green fluorescent protein fusion protein and pull-down analysis. The glutathione *S*-transferase (GST)–SOCS3–green fluorescent protein (GFP) fusion protein was prepared according to our previous method (8, 17). Briefly, the *SOCS3* gene cloned from RAW264.7 cells was subcloned into plasmid pGEX-6P-GFP to generate the GST-SOCS3-GFP or GST-GFP fusion proteins. GST-SOCS3-GFP was bound to a GST Trap FF column, and detergent extracts of 2×10^6 DCs were passed over the column. After extensive washing, the compound was eluted with 50 mmol/L Tris-HCl and 10 mmol/L reduced glutathione at pH 8.0. Eluates were analyzed by Western blot.

Binding of SOCS3 to phosphopeptides from M2-PK. Phosphotyrosine-containing peptides from M2-PK were synthesized and labeled using 5-carboxyfluorescein (FAM) by Shanghai Science Peptide Biological Technology Co. Ltd. GST-SOCS3 fusion proteins were covalently immobilized onto beads of glutathione agarose (Amersham Biosciences). Then, the immobilized protein was incubated with 5-FAM–labeled phosphopeptide solubilized in 1 mL of 50 mmol/L sodium phosphate (pH 7.5) containing 150 mmol/L NaCl, 2 mmol/L DTT, and 0.2% (v/v) Tween 20. Binding of 5-FAM–labeled phosphorylated and nonphosphorylated peptides was detected using fluorescence intensity, which was measured with a DyNA Quant 200 Fluorometer (Hoefer Pharmacia Biotech, Inc.) using an excitation filter of 365 nm and an emission filter of 510 nm.

Plasmid construction. pcDNASOCS3, pcDNAM2-PK, and the mutant form of M2-PK, pcDNAM2-PKΔ105, were prepared using the pcDNATOPOV5/His kit according to the manufacturer's protocol (Invitrogen). To produce lentiviruses containing SOCS3, M2-PK, or M2-PKΔ105, the genes for these proteins were first subcloned into PLenti6/V5/D vectors from pcDNA plasmids using the PLenti6/V5/D-Topo kit according to the recommended protocol (Invitrogen). Lentiviruses were generated by cotransfecting 293T cells together with packaging vectors based on the company's instructions (Invitrogen). These packaged lentiviruses expressing SOCS3, M2-PK, or M2-PKΔ105, as well as control scrambled lentiviruses, were used to transduce DCs. Primers used to clone SOCS3 include 5′-atggtcacccacagcaagtttcc-3′ (forward) and 5′-aagtggagcatcatactgatccagg-3′ (reverse). Primers used to clone M2-PK were 5′-atgccgaagccacacagtgaagc-3′ (forward) and 5′-aggtacaggcactacacgcatgg-3′ (reverse).

For mutant M2-PKΔ105, four primers were used: 5′-atgccgaagccacacagtgaagc-3′, 5′-aggtacaggcactacacgcatgg-3′, 5′-gcatctgatcccattctcGGGgtcctgttg-3′ and 5′-gagccaccgcaacaggacgCCCgtagagaatg-3′ (capital letters, mutated 105 amino acid residues).

Small interfering RNA (siRNA) sequences used for silencing murine SOCS3 (mSOCS3) were designed using the protocol described by Ambion.[4] The specific sequences of mSOCS3 that were targeted included sequence 1 (AAGAGAGCTTACTACATCTAT) and sequence 2 (AAGAACCTACGCATCCAGTGT). The nonsilencing control siRNA was an irrelevant siRNA with random nucleotides ACUATCUAAGUUACTACCCCTT. Sequences were synthesized, annealed, and used to transfect the cells. The mouse genome database was searched (BLAST) to ensure that the sequence would not target any other gene transcript. Cells were transfected with

[4] http://www.ambion.com

Published OnlineFirst December 8, 2009; DOI: 10.1158/0008-5472.CAN-09-2970

the siRNAs using the Nucleofector Device (Amaxa) according to the manufacturer's protocol.

Measurement of M2-PK activity and expression. M2-PK activity was measured according to the reported method (18) with a M2-PK activity detection kit (Nanjing Jiancheng Bioengineering Institute, Nanjing, China) using a continuous assay coupled to lactate dehydrogenase. The change in absorbance at 340 nm caused by the oxidation of NADH was measured using a spectrophotometer (Perkin-Elmer, Inc.). M2-PK expression of cells was measured using a commercially available mouse pyruvate kinase M2-PK ELISA kit (USCN Life Science & Technology). The absorbance of each well was determined using a microplate reader at 450 nm. The M2-PK concentration was derived from the standard curve.

Reverse transcription-PCR analysis. Total cellular RNA was prepared using the Trizol Reagent (Invitrogen) followed by RNA cleanup with the RNeasy Mini kit (Qiagen) as recommended by the manufacturer. Reverse transcription-PCR (RT-PCR) was performed using SuperScript one-step RT-PCR with Platinum Taq according to the provided protocol (Invitrogen). The following primers were used: SOCS3, 5′-ATGGTCACCCACAGCAAGTTTCC-3′ (forward) and 5′-AAGTGGAGCATCATAAACTCCC-3′ (reverse); glyceraldehyde-3-phosphate dehydrogenase (GAPDH), 5′-ATGGTGAAGGTCGGTGTGAACGGATTTGGC-3′ (forward) and 5′-CATCGAAGGTGGAAGAGTGGGAGTTGCTGT-3′ (reverse).

Western blotting analysis. Cells were harvested and washed twice with cold PBS, and 1×10^6 pelleted cells

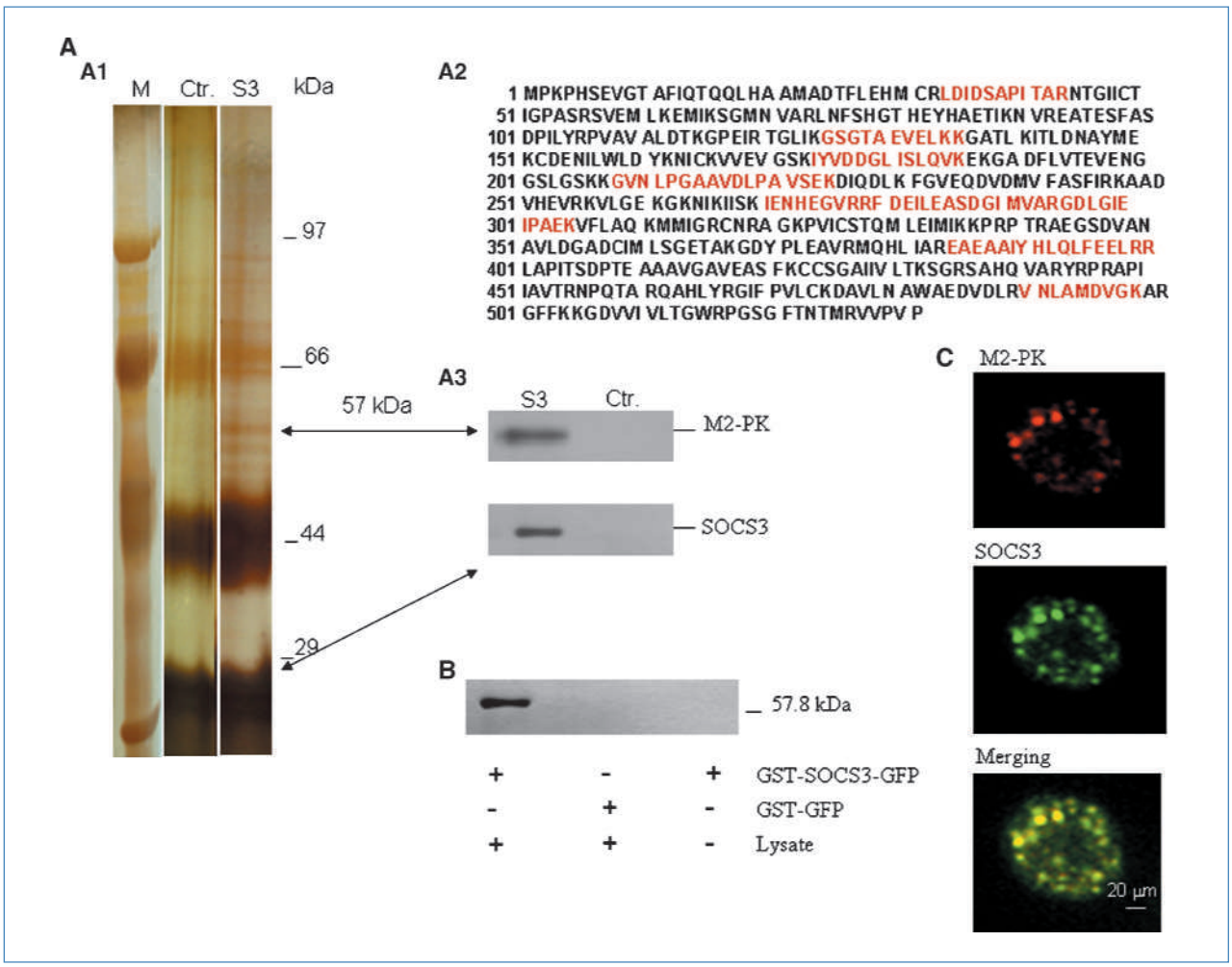

Figure 1. The interaction of SOCS3 with M2-PK. *A,* identification of a novel partner of SOCS3. *A1,* immunoprecipitation and silver staining analysis. *M,* protein marker; *Ctr.,* control empty plasmid–transfected 1D8 ovarian carcinoma cells; *S3,* SOCS3 plasmid–transfected 1D8 ovarian carcinoma cells. *A2,* MALDI-TOF/TOF-MS/MS analysis of the 57-kDa band. *Bold red,* matched peptides. *A3,* Western blot analysis of the immunoprecipitation. Western blot analysis of the immunoprecipitation was performed using anti-mouse M2-PK or anti-mouse SOCS3 antibodies. *B,* pull-down analysis of the binding of M2-PK to SOCS3. M2-PK from the lysates of mouse DCs was bound to GST-SOCS3-GFP but not to GST-GFP. *C,* localization of endogenous SOCS3 and M2-PK in BMDCs. BMDCs were grown on glass coverslips and then washed with PBS, fixed with 3.7% paraformaldehyde, and permeabilized with 1% (v/v) Triton X-100 for 20 min. The cells were incubated for 20 min at room temperature with rabbit anti–M2-PK and goat anti-SOCS3 antibodies, stained with PE-labeled donkey polyclonal antibodies against the rabbit IgG antibodies and FITC-labeled rabbit anti-goat IgG antibodies, and then examined by confocal fluorescence microscopy.

Published OnlineFirst December 8, 2009; DOI: 10.1158/0008-5472.CAN-09-2970

were disrupted on ice in lysis buffer (50 mmol/L HEPES, 150 mmol/L NaCl, 5 mmol/L EDTA, 1 mmol/L $NaOV_4$, 0.5% Triton, 0.1 μg/μL pepstatin, 0.1 μg/μL antipain, 0.1 μg/μL aprotinin, 2 mmol/L phenylmethylsulfonyl fluoride). Proteins were separated on a 10% denaturing SDS polyacrylamide gel and transferred to a polyvinylidene difluoride membrane (Millipore). The membrane was saturated for 1 h at room temperature in PBS/0.05% Tween 20 supplemented with different concentrations of nonfat dried milk (Sigma-Aldrich). Hybridizations with primary antibodies were carried out for 1 h at room temperature in blocking buffer. The protein-antibody complexes were detected using peroxidase-conjugated secondary antibodies (Boehringer Mannheim) and ECL (Amersham).

Hypoxic culture and ATP assay. Cells were incubated at 37°C under hypoxia (5% CO_2, balanced N_2) in a modular incubation chamber according to a reported method (7). ATP levels in the cells were assayed using ATP Bioluminescent Assay kit (Sigma-Aldrich) according to the protocols described by the company. The light emission was measured using the Kodak Imaging System. ATP levels were determined from the standard curve.

In vivo *experiments.* *In vivo* experiments were designed to investigate effect of interaction of SOCS3 with M2-PK on DC-based immunotherapy against tumors according to the reported protocol (19). LLC cells (0.5×10^6 in 100 μL of saline) were inoculated s.c. into the back of C57BL/6 mice. Tumors were allowed to develop for 9 d and mice were then randomly divided into different experimental groups (six mice per group) and then treated with intratumoral injections of the transduced DCs, respectively. The groups treated with only PBS or nontreated DCs were used as controls.

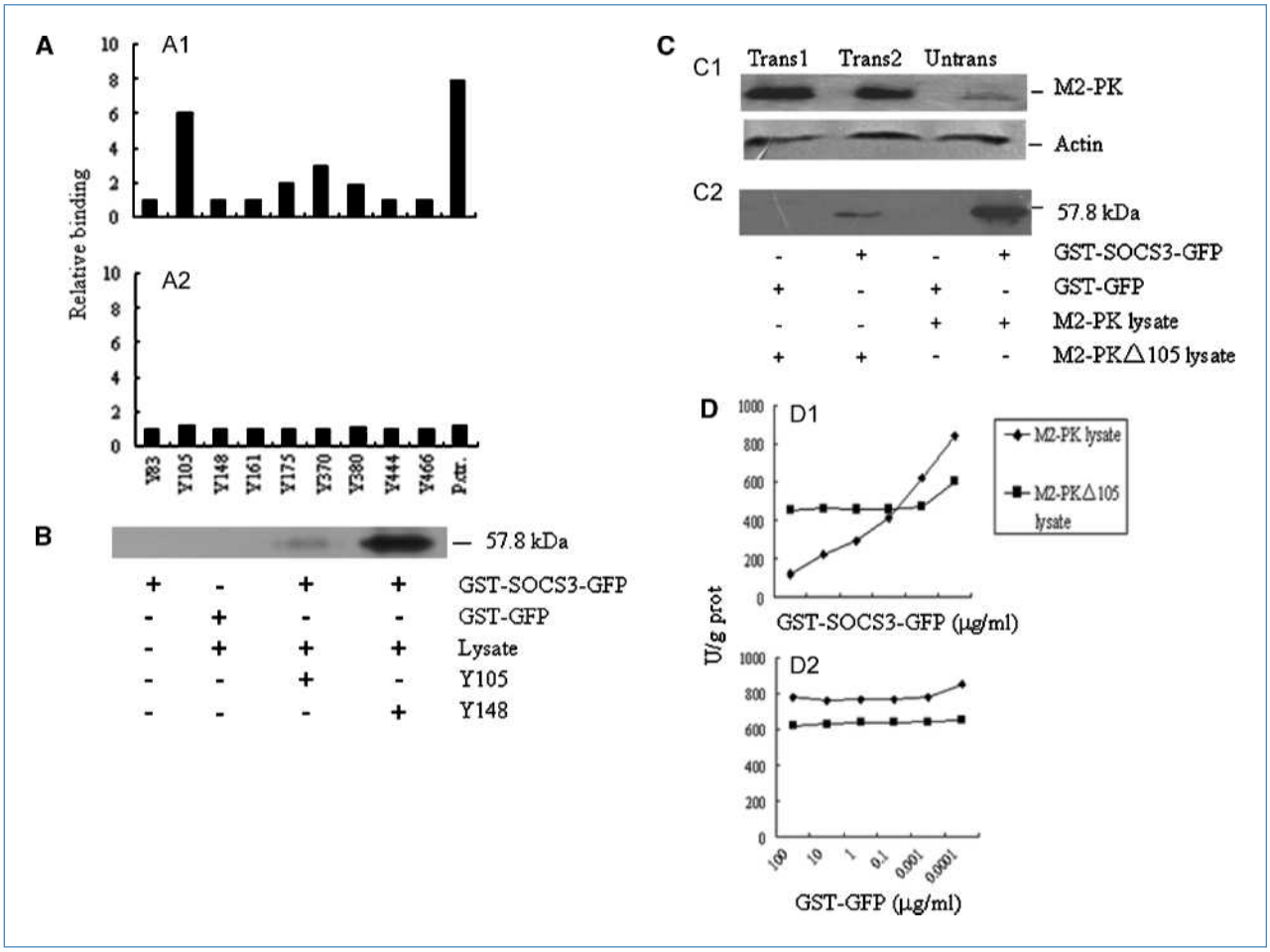

Figure 2. M2-PK pY105 is a SOCS3 binding site. *A,* remarkable binding of SOCS3 with phosphopeptide Y105 but not other phosphopeptides (*A1*) or nonphosphopeptides (*A2*). Relative binding results are in reference to the results with glutathione agarose alone. *B,* suppression of the Y105, but not Y148, peptide on the binding of SOCS3 to M2-PK in the pull-down analysis. *C,* binding of SOCS3 with M2-PK but not with mutant M2-PKΔ105. *C1,* lysates of RAW264.7 cells transfected with M2-PK (*Trans1*) or M2-PKΔ105 (*Trans2*) and untransfected RAW264.7 cells (*Untrans*) were analyzed by Western blotting with anti-mouse M2-PK antibodies. *C2,* binding of the SOCS3 fusion protein with M2-PK but not with M2-PKΔ105. *D,* SOCS3 inhibited the M2-PK activity of cell lysates of M2-PK–transfected cells. The different concentrations of either the SOCS3 fusion protein (GST-SOCS3-GFP; *D1*) or the control protein (GST-GFP; *D2*) were added to the lysates of RAW264.7 cells transfected with either M2-PK (*M2-PK lysate*) or M2-PKΔ105 (*M2-PKΔ105 lysate*), respectively. M2-PK activity was measured according to the published metabolic method as described in Materials and Methods. *U/g prot,* units of pyruvate activity per gram of tissue.

Published OnlineFirst December 8, 2009; DOI: 10.1158/0008-5472.CAN-09-2970

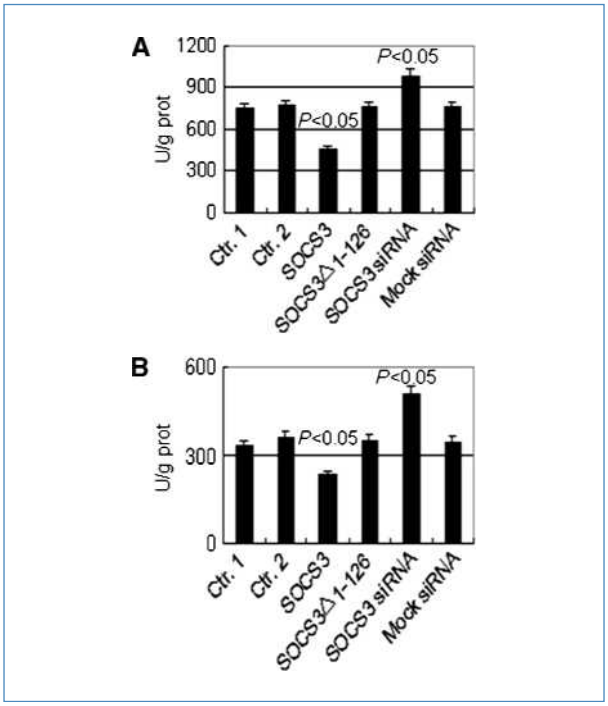

Figure 3. SOCS3 regulates M2-PK activity. The effect of SOCS3 on M2-PK activity in RAW264.7 cells (*A*) and BMDCs (*B*). M2-PK activity was inhibited by ectopic SOCS3, whereas silencing SOCS3 promoted M2-PK activity. Additionally, the deletion of amino acids 1 to 126 of SOCS3 could abolish the effect of SOCS3 on M2-PK activity. One unit is equal to a change of 1 μmol PEP to pyruvate per minute by 1 g of tissue. *Ctr.1,* untransduced RAW264.7 cells or DCs; *Ctr.2, SOCS3* and *SOCS3Δ1-126*, control lentivirus–transduced, SOCS3 lentivirus–transduced, or SOCS3Δ1-126 lentivirus–transduced RAW264.7 cells (*A*) or BMDCs (*B*), respectively; *SOCS3 siRNA* and *mock siRNA*, SOCS3-targeting siRNA–transfected or control irrelevant siRNA–transfected RAW264.7 cells (*A*) or BMDCs (*B*), respectively.

Immunohistochemistry. Tumor tissue samples from LLC-bearing mice were harvested and placed in the OCT compound (Tissue-Tek) and stored at −80°C. Cryostat sections (5 μm) were fixed in cold acetone for 15 min. Slides were washed with PBS and incubated for 1 h at room temperature with the appropriate dilutions of PE-labeled anti-CD4, anti-CD8, or anti-CD11c antibodies or stained with 4′,6-diamidino-2-phenylindole and then observed under a fluorescence microscope.

Statistical analysis. The Student's *t* test was used for the statistical analysis and a 95% confidence limit was taken to be significant and was defined as $P < 0.05$.

Results

Interaction of SOCS3 with M2-PK. We have previously reported the binding of SOCS3 with TYK2 by immunoprecipitating the lysates of SOCS3-transfected RAW264.7 cells (8). To look for additional potential partner(s) of SOCS3, we performed another immunoprecipitation of the lysates of SOCS3-transfected 1D8 ovarian carcinoma cells. At least five bands between 44 and 66 kDa were precipitated from the lysates, whereas these bands were not observed in the lysates of control 1D8 cells transfected with an empty vector or with the isotype-matched antibody control (Fig. 1*A1*; data not shown), implying that new SOCS3 partner(s) was found. Unfortunately, these bands were not clearly identified by peptide mass fingerprinting. However, when the fragmentation patterns of the tryptic peptide molecular ions were further analyzed by TOF-MS/MS, seven peptides were identified as having a protein sequence that was consistent with M2-PK (Fig. 1*A2*). Combining the protein accession number from National Center for Biotechnology Information, molecular mass, MASCOT protein score, and confidence index, we finally identified a novel SOCS3 partner, M2-PK. The association between SOCS3 and M2-PK was further confirmed by Western blot analysis also (Fig. 1*A3*).

To investigate the interaction of SOCS3 with M2-PK in DCs, the lysates of BMDCs were passed over glutathione-Sepharose beads that had been precoated with GST-SOCS3-GFP. The bound proteins were separated and analyzed by Western blotting using a M2-PK monoclonal antibody. As illustrated in Fig. 1*B*, M2-PK from the lysates of BMDCs was bound to GST-SOCS3-GFP but not to GST-GFP. Both proteins displayed a similar, mostly perinuclear staining as well as showed an overlap in subcellular distribution, as seen by the appearance of yellow dots when the staining was superimposed (Fig. 1*C*). Thus, these results suggest that SOCS3 may bind to M2-PK in tumor cells as well as DCs.

The p105 tyrosine residue of M2-K (M2-K pY105) is located in a SOCS3 binding site. Because SOCS3 has a central SH2 domain that targets the protein to phosphorylate tyrosine residues, thus causing it to interfere with signaling (20), we hypothesized that an interaction between SOCS3 and M2-PK might occur via the SOCS3 binding site of M2-PK, which contains tyrosine residues (Supplementary Fig. S1). To find the SOCS3 binding sequence in M2-PK, we first designed and synthesized peptides containing phosphorylated tyrosine residues based on the murine M2-PK protein sequence (Supplementary Fig. S2). In all of the phosphorylated peptides examined, only Y105 (pYRPVAVAL), with the amino acid residue valine at the +3 position from the phosphotyrosine, exhibited a better optimized interaction with SOCS3 (Fig. 2*A1*). Several other phosphorylated peptides, such as Y161 and Y466, did not show similar binding. Additionally, consistent with other reports (21), SOCS3 did not bind to the nonphosphorylated peptides (Fig. 2*A2*). As the positive control, peptide pYSTVVHSG (21), a sequence containing the Y757 docking site of murine gp130, also showed a remarkable tendency to bind SOCS3 (Fig. 2*A1*).

The interaction between M2-PKpY105 and SOCS3 was also confirmed by pull-down analysis. Binding of SOCS3 to M2-PK was remarkably inhibited by Y105 (pYRPVAVAL) peptides but not by control pY148 peptides (Fig. 2*B*). To further determine the role of the pY105 tyrosine residue, we used glycine to replace the M2-PKp105 tyrosine residue to produce mutant M2-PK (M2-PKΔ105). As shown in Fig. 2*C*, M2-PK, but not M2-PKΔ105, was bound by the SOCS3 fusion protein. Furthermore, the SOCS3 fusion protein remarkably inhibited the M2-PK activity of the

Published OnlineFirst December 8, 2009; DOI: 10.1158/0008-5472.CAN-09-2970

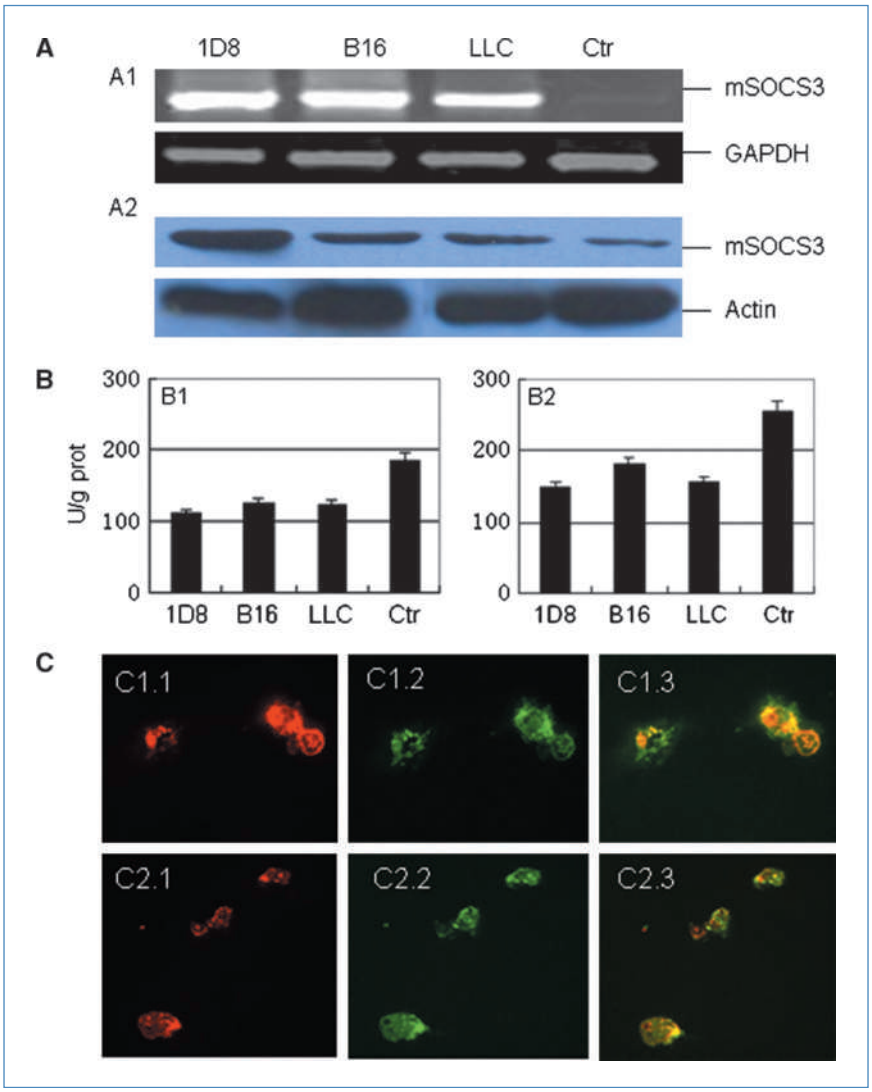

Figure 4. Tumor-associated DCs have reduced M2-PK activity. *A,* tumor-associated DCs expressed higher levels of SOCS3. Transcripts and protein levels of SOCS3 were determined by RT-PCR (*A1*) and by Western blot analysis (*A2*), respectively, as described in Supplementary Materials and Methods. Mouse monoclonal anti-SOCS3 antibodies were used for the Western blot analysis. *B,* lower levels of pyruvate kinase activity in the DCs isolated from different types of tumor tissues (*B1*) and in the DCs isolated from the spleens of tumor-bearing mice (*B2*). DCs from different tissues were isolated using anti-CD11c magnetic beads according to the protocol described by the company (Invitrogen). *C,* tumor tissue–derived DCs lost typical morphology. DCs from disease-free lymph node tissue (*C1*) and 18D ovarian carcinoma tissue (*C2*) were isolated by anti-CD11c magnetic beads. The cells were stained with PE-labeled anti-CD80 antibodies (*C1.1* and *C2.1*) and FITC-labeled anti-CD11c antibodies (*C1.2* and *C2.2*), and then observed under fluorescence microscopy. *C1.3,* merged image of *C1.1* and *C1.2*; *C2.3,* merged image of *C2.1* and *C2.2*. 1D8, B16, LLC, and Ctr are, respectively, DCs from the spleens of mice bearing 1D8 ovarian carcinoma, B16 melanoma, or LLC or from the spleens of disease-free mice.

lysates from the M2-PK–transfected RAW264.4 cells but not from M2-PKΔ105–transfected RAW264.7 cells (Fig. 2*D1*). As a control, the GST-GFP fusion protein did not significantly suppress M2-PK activity (Fig. 2*D2*). Thus, our results suggest that the p105 tyrosine residue of M2-PK (M2-PK pY105) may be part of the SOCS3 binding site.

SOCS3 inhibits M2-PK activity. To investigate the effect of intracellular SOCS3 on M2-PK activity, we first produced lentivirus-based structures to transduce monocyte/macrophage RAW264.7 cells or BMDCs. The high efficiency of SOCS3 transduction could be shown by immunofluorescence with an anti–V5 tag-specific monoclonal antibody (Supplementary Fig. S3). As expected, ectopic SOCS3 in both transduced RAW264.7 cells and BMDCs remarkably decreased M2-PK activity as compared with nontransduced and control lentivirus–transduced cells (Fig. 3*A* and *B*). Because the NH_2-terminal SH2 domain of SOCS3 plays a critical role in determining the interaction of SOCS3 with its phosphotyrosine binding site (21), we deleted the SH2 region of SOCS3 (NH_2-terminal 1–126 region, SOCS3Δ1-126) and observed the effect of SOCS3Δ1-126 on M2-PK activity. Indeed, M2-PK activity in the SOCS3Δ1-126–transduced cells did not exhibit a significant change as compared with control (Fig. 3*A* and *B*), suggesting that the SOCS3 SH2 region plays a critical role in mediating the suppression of M2-PK activity.

We next used knockdown techniques to investigate the effect of silencing SOCS3 on the activity of M2-PK in both RAW264.7 cells and BMDCs. SOCS3-targeting siRNA, but not the control siRNA, reduced the levels of SOCS3 transcript and protein without affecting GAPDH transcript or actin protein levels (Supplementary Fig. S4). M2-PK activity in SOCS3-targeting siRNA–transfected RAW264.7 cells or BMDCs was remarkably higher than that in control-transfected RAW264.7 cells or BMDCs ($P < 0.05$; Fig. 3*A* and *B*), further supporting a role for SOCS3 in regulating M2-PK activity. Notably, the levels of M2-PK expression were similar in the differently treated cells (Supplementary Fig. S5), indicating that SOCS3 does not affect the expression of M2-PK.

Published OnlineFirst December 8, 2009; DOI: 10.1158/0008-5472.CAN-09-2970

Tumor-associated DCs with higher levels of SOCS3 have decreased M2-PK activity. We previously reported that, in addition to IL-6 and LPS, tumor-associated factors could also upregulate SOCS3 expression in murine BMDCs (8). The isolated DCs from the spleens of mice bearing a 1D8 ovarian carcinoma (1D8), B16 melanoma, or LLC also expressed higher levels of SOCS3 than DCs from the spleens of disease-free mice (Fig. 4*A*). Thus, the DCs in tumor

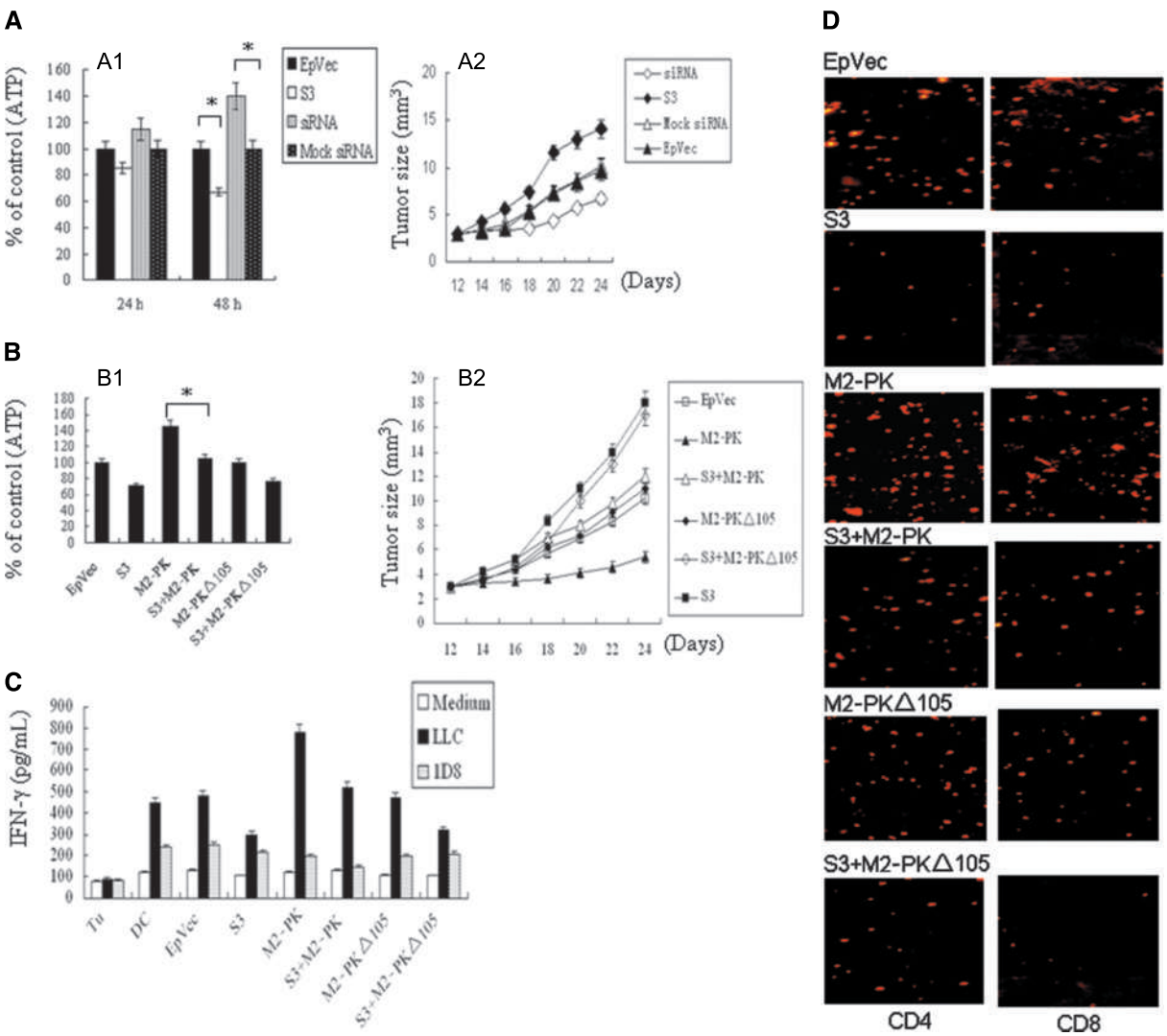

Figure 5. Interaction of SOCS3 with M2-PK impairs DC-based immunotherapy against tumors. *A,* tumors grew faster in mice immunized by SOCS3-transduced DCs, whereas silencing of SOCS3 significantly inhibited tumor growth. $P < 0.05$ is defined as significant. *A1,* lower level of ATP in SOCS3-transduced DCs under hypoxic conditions. *A2,* tumor growth in mice immunized by SOCS3-transduced DCs. *, $P < 0.05$. *B,* interaction of SOCS3 with M2-PK impairs DC-based immunotherapy against tumors. *B1,* SOCS3 affected the M2-PK–mediated ATP generation under hypoxic conditions. ATP levels were measured after transduction for 48 h. *, $P < 0.05$. *B2,* M2-PK–transduced DCs significantly improved DC-based immunotherapy against LLC, but the LLC tumor grew remarkably faster in mice vaccinated with both SOCS3-transduced and M2-PK–transduced DCs than that in mice vaccinated with only M2-PK–transduced DCs. *C,* lymph node cells isolated from mice intralesionally vaccinated with M2-PK–transduced DCs released higher levels of IFN-γ than lymph node cells from mice immunized with DCs cotransduced with both SOCS3 and M2-PK. Draining lymph node cells were isolated on day 24 after tumor injection from each experimental group. The cells (1×10^6/mL) were stimulated with irradiated LLC cells (0.2×10^5) or irradiated control 1D8 ovarian carcinoma cells (0.2×10^5) and incubated in 24-well tissue culture plates for 48 h. The supernatants were collected and evaluated for the production of IFN-γ using an ELISA kit (R&D Systems). $P < 0.05$ is defined as significant. *Medium,* no stimulated cells were added. *D,* CD4 and CD8 T-cell infiltration was remarkably reduced in the group of mice intralesionally vaccinated with DCs cotransduced with SOCS3 and M2-PK. *EpVec,* control lentivirus–transduced DCs; *siRNA* and *mock siRNA*, SOCS3-targeting siRNA or the irrelevant siRNA-transfected BMDCs, respectively; *S3, M2-PK, S3+M2-PK, M2-PKΔ105*, and *S3+M2-PKΔ105*, SOCS3 lentivirus–transduced, M2-PK lentivirus–transduced, SOCS3 and M2-PK lentivirus–transduced, M2-PKΔ105 lentivirus–transduced, or SOCS3 and M2-PKΔ105 lentivirus–transduced DCs, respectively.

Published OnlineFirst December 8, 2009; DOI: 10.1158/0008-5472.CAN-09-2970

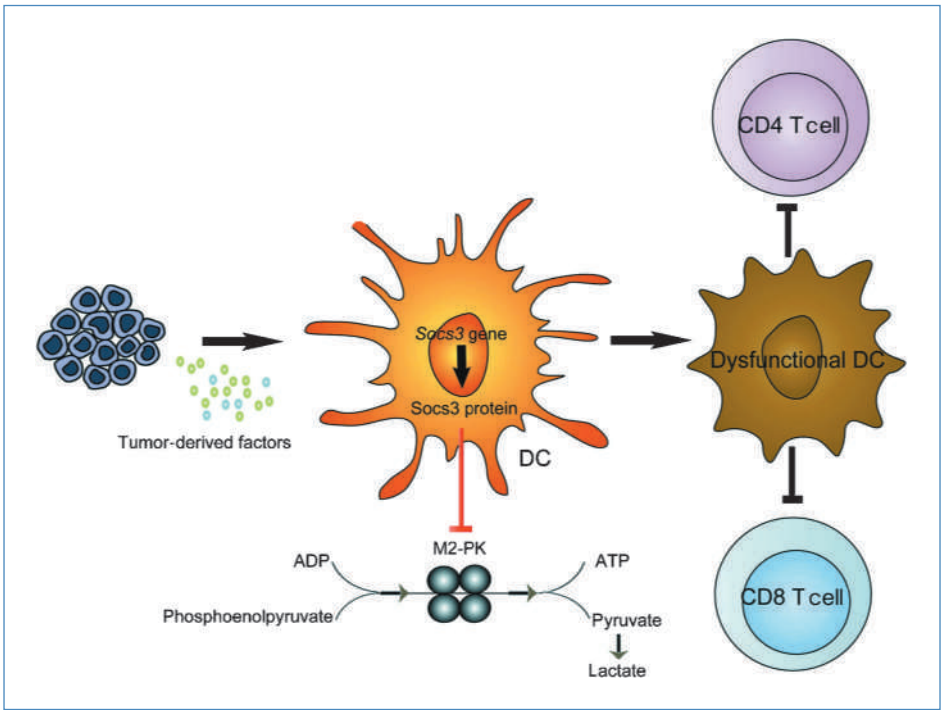

Figure 6. Tumor-associated DCs impair immune responses against tumors via an interaction between SOCS3 and M2-PK. While DCs are in the tumor environment, SOCS3 expression is upregulated by tumor-derived factors. The upregulated SOCS3 may interact with M2-PK to decrease ATP production by downregulating M2-PK activity, which ultimately causes DC dysfunction. These dysfunctional DCs have a reduced ability to present antigens.

environments may also have reduced pyruvate kinase activity. As predicted, the DCs isolated from tumor tissues or spleens of mice bearing 1D8, B16, or LLC showed reduced pyruvate kinase activity as compared with the DCs isolated from the spleens of disease-free mice (Fig. 4*B*). Because DCs use the glycolytic pathway as the main source of energy in the absence of oxygen (22), we further hypothesized that the upregulated SOCS3 could be involved in the induction of altered DC function by interacting with M2-PK. Indeed, DCs isolated from tumor tissues lost the typical morphology seen in DCs isolated from healthy tissue (Fig. 4*C*). However, the levels of M2-PK expression were similar in all of the DCs (Supplementary Fig. S6), indicating that reduced M2-PK activity in the tumor-associated DCs was not caused by change of M2-PK expression.

The interaction of SOCS3 with M2-PK impairs DC-based immunotherapy against tumors. Because M2-PK plays a critical role in ATP production in the absence of oxygen, interaction of SOCS3 with M2-PK may decrease ATP production to affect the function of DCs. SOCS3 transduction indeed declined the generation of M2-PK–mediated ATP in DCs under hypoxic conditions (Fig. 5). Importantly, the interaction between SOCS3 and M2-PK affected DC-based immunotherapy against tumor. As shown in Fig. 5, M2-PK alone–transduced DCs significantly improved DC-based immunotherapy against LLC as compared with control scrambled lentivirus–transduced or M2-PKΔ105 lentivirus–transduced DCs ($P < 0.05$), whereas, consistent with our previous finding (8), SOCS3-transduced DCs remarkably reduced DC-based immunotherapy against tumor (Fig. 5*A* and *B*). However, although both SOCS3-cotransduced and M2-PK–cotransduced DCs were used to immunize mice (Supplementary Fig. S7), SOCS3 remarkably impaired the role of M2-PK in DC-based immunotherapy against LLC. LLC tumor grew remarkably faster in mice vaccinated with SOCS3-cotransduced and M2-PK–cotransduced DCs than that in mice vaccinated with only M2-PK–transduced DCs ($P < 0.05$; Fig. 5*B*). The interaction of SOCS3 with M2-PK also affected the production of tumor-specific T cells. Lymph node cells isolated from mice intralesionally vaccinated with M2-PK–transduced DCs released higher levels of IFN-γ, whereas lymph node cells from mice immunized with DCs cotransduced with both SOCS3 and M2-PK only produced a low level of IFN-γ ($P < 0.05$; Fig. 5*C*). Decreased $CD4^+$ and $CD8^+$ T-cell infiltration in these tumors was also observed in the group of mice intralesionally vaccinated with DCs cotransduced with SOCS3 and M2-PK as compared with those vaccinated with only M2-PK–transduced DCs (Fig. 5*D*).

Discussion

Similar to other cells, antigen-presenting cells such as DCs also use glycolysis as a metabolic pathway to generate ATP, and the use of glycolysis is considered one of the most fundamental metabolic alterations in the absence of oxygen (22). When M2-PK is inhibited by phosphorylation, phosphoenolpyruvate (PEP) is prevented from being converted to pyruvate, a process that is used to convert ADP to ATP (23). In normal cells, M2-PK is mainly high active tetrameric form, whereas M2-PK isoenzyme found in tumor cells is usually less active dimeric form of M2-PK to accumulate precursors for synthetic

Published OnlineFirst December 8, 2009; DOI: 10.1158/0008-5472.CAN-09-2970

processes (24, 25). In this study, we found that M2-PK is a partner of SOCS3 and show that M2-PK activity can be inhibited by the direct interaction of SOCS3 with M2-PK. Importantly, we also found that DCs isolated from tumor tissues have upregulated SOCS3 expression and downregulated M2-PK activity. Moreover, the interaction of SOCS3 with M2-PK remarkably impairs DC-based immunotherapy against tumors. Thus, our results suggest a new mechanism for DCs in the tumor microenvironment by which SOCS3 may induce DC dysfunction (Fig. 6). SOCS3 expression in DCs is upregulated by tumor-derived factors. The upregulated SOCS3 may interact with M2-PK to decrease ATP production via the downregulation of M2-PK activity, which ultimately causes DC dysfunction. These dysfunctional DCs have a reduced ability to present antigens.

SOCS3 plays an important role in inducing DC dysfunction and causing immune tolerance. It is a critical regulator of cytokine signaling and the Janus-activated kinase/signal transducer and activator of transcription pathway (26–29). SOCS3 can act as a negative regulator of inflammatory responses (30–32). Recently, we (8) and others (33) found that the intracellular delivery of SOCS3 significantly reduces the production of inflammatory cytokines. DCs transduced with SOCS3 exhibit a tolerogenic/DC2 phenotype (34). Injection of SOCS3-transduced DCs significantly suppresses experimental autoimmune encephalomyelitis. SOCS3-transgenic mice exhibit enhanced Th2 differentiation (30, 31). SOCS3 proteins have been shown to modulate macrophage function and negatively regulate LPS-induced macrophage activation (35).

M2-PK, a key enzyme in the glycolysis metabolic pathway, undergoes very complex regulation. M2-PK activity may be downregulated by the direct interaction of SOCS3 with M2-PK. Other studies have shown that M2-PK activity in tumor cells is also regulated by the direct interaction of M2-PK with several oncoproteins. The transforming factor of Rous sarcoma virus, pp60v-src kinase, has tyrosine kinase–specific activity and phosphorylates M2-PK at a tyrosine residue to reduce M2-PK activity (23, 36). The serine/threonine kinase A-Raf directly binds to M2-PK to regulate the pyruvate kinase (25). Furthermore, pyruvate kinase is also regulated indirectly by insulin and glucagons, which control protein kinase activity.

Disclosure of Potential Conflicts of Interest

No potential conflicts of interest were disclosed.

Grant Support

National Natural Science Foundation of China grants 30771967 and 30872315; Ministry of Science and Technology of the People's Republic of China grants 06C26211200695, 2008AA02Z129, and 2006AA020502; and Tianjin Municipal Science and Technology Commission grants 07JCZDJC03300 and 06ZHCXSH04800.

The costs of publication of this article were defrayed in part by the payment of page charges. This article must therefore be hereby marked *advertisement* in accordance with 18 U.S.C. Section 1734 solely to indicate this fact.

Received 8/19/09; revised 10/2/09; accepted 10/22/09; published OnlineFirst 12/8/09.

References

1. Huang AY, Golumbek P, Ahmadzadeh M, Jaffee E, Pardoll D, Levitsky H. Bone marrow-derived cells present MHC class I-restricted tumour antigens in priming of antitumour immune responses. Ciba Found Symp 1994;187:229–40.
2. Armstrong TD, Pulaski BA, Ostrand-Rosenberg S. Tumor antigen presentation: changing the rules. Cancer Immunol Immunother 1998;46:70–4.
3. Gottfried E, Kreutz M, Mackensen A. Tumor-induced modulation of dendritic cell function. Cytokine Growth Factor Rev 2008;19:65–77.
4. Bennaceur K, Chapman J, Brikci-Nigassa L, Sanhadji K, Touraine JL, Portoukalian J. Dendritic cells dysfunction in tumour environment. Cancer Lett 2008;272:186–96.
5. Liao YP, Schaue D, McBride WH. Modification of the tumor microenvironment to enhance immunity. Front Biosci 2007;12:3576–600.
6. Qu X, Yang MX, Kong BH, et al. Hypoxia inhibits the migratory capacity of human monocyte-derived dendritic cells. Immunol Cell Biol 2005;83:668–73.
7. Turner L, Scotton C, Negus R, Balkwill F. Hypoxia inhibits macrophage migration. Eur J Immunol 1999;29:2280–7.
8. Zeng B, Li H, Liu Y, Zhang Z, Zhang Y, Yang R. Tumor-induced suppressor of cytokine signaling 3 inhibits toll-like receptor 3 signaling in dendritic cells via binding to tyrosine kinase 2. Cancer Res 2008;68:5397–404.
9. Babon JJ, McManus EJ, Yao S, et al. The structure of SOCS3 reveals the basis of the extended SH2 domain function and identifies an unstructured insertion that regulates stability. Mol Cell 2006;22:205–16.
10. Hilton DJ. Negative regulators of cytokine signal transduction. Cell Mol Life Sci 1999;55:1568–77.
11. Hirano T, Murakami M. Grasp a pTyr-peptide by its SOCS. Dev Cell 2006;10:542–4.
12. Yoshimura A, Naka T, Kubo M. SOCS proteins, cytokine signalling and immune regulation. Nat Rev Immunol 2007;7:454–65.
13. Naka T, Fujimoto M, Tsutsui H, Yoshimura A. Negative regulation of cytokine and TLR signalings by SOCS and others. Adv Immunol 2005;87:61–122.
14. Cassatella MA, Gasperini S, Bovolenta C, et al. Interleukin-10 (IL-10) selectively enhances CIS3/SOCS3 mRNA expression in human neutrophils: evidence for an IL-10-induced pathway that is independent of STAT protein activation. Blood 1999;94:2880–9.
15. Yang R, Murillo FM, Cui H, et al. Papillomavirus-like particles stimulate murine bone marrow-derived dendritic cells to produce α interferon and Th1 immune responses via MyD88. J Virol 2004;78:11152–60.
16. Roby KF, Taylor CC, Sweetwood JP, et al. Development of a syngeneic mouse model for events related to ovarian cancer. Carcinogenesis 2000;21:585–91.
17. Yang R, Yutzy WHT, Viscidi RP, Roden RB. Interaction of L2 with β-actin directs intracellular transport of papillomavirus and infection. J Biol Chem 2003;278:12546–53.
18. Malcovati M, Valentini G. AMP- and fructose 1,6-bisphosphate-activated pyruvate kinases from *Escherichia coli*. Methods Enzymol 1982;90:170–9.
19. Zhong H, Han B, Tourkova IL, et al. Low-dose paclitaxel prior to intratumoral dendritic cell vaccine modulates intratumoral cytokine network and lung cancer growth. Clin Cancer Res 2007;13:5455–62.
20. Endo TA, Masuhara M, Yokouchi M, et al. A new protein containing an SH2 domain that inhibits JAK kinases. Nature 1997;387:921–4.
21. De Souza D, Fabri LJ, Nash A, Hilton DJ, Nicola NA, Baca M. SH2

Published OnlineFirst December 8, 2009; DOI: 10.1158/0008-5472.CAN-09-2970

domains from suppressor of cytokine signaling-3 and protein tyrosine phosphatase SHP-2 have similar binding specificities. Biochemistry 2002;41:9229–36.
22. Pelicano H, Martin DS, Xu RH, Huang P. Glycolysis inhibition for anticancer treatment. Oncogene 2006;25:4633–46.
23. Weernink PA, Rijksen G, Mascini EM, Staal GE. Phosphorylation of pyruvate kinase type K is restricted to the dimeric form. Biochim Biophys Acta 1992;1121:61–8.
24. Mazurek S, Boschek CB, Hugo F, Eigenbrodt E. Pyruvate kinase type M2 and its role in tumor growth and spreading. Semin Cancer Biol 2005;15:300–8.
25. Mazurek S, Drexler HC, Troppmair J, Eigenbrodt E, Rapp UR. Regulation of pyruvate kinase type M2 by A-Raf: a possible glycolytic stop or go mechanism. Anticancer Res 2007;27:3963–71.
26. Lang R, Pauleau AL, Parganas E, et al. SOCS3 regulates the plasticity of gp130 signaling. Nat Immunol 2003;4:546–50.
27. Yasukawa H, Ohishi M, Mori H, et al. IL-6 induces an anti-inflammatory response in the absence of SOCS3 in macrophages. Nat Immunol 2003;4:551–6.
28. Croker BA, Metcalf D, Robb L, et al. SOCS3 is a critical physiological negative regulator of G-CSF signaling and emergency granulopoiesis. Immunity 2004;20:153–65.
29. Kimura A, Kinjyo I, Matsumura Y, et al. SOCS3 is a physiological negative regulator for granulopoiesis and granulocyte colony-stimulating factor receptor signaling. J Biol Chem 2004;279:6905–10.
30. Yamamoto K, Yamaguchi M, Miyasaka N, Miura O. SOCS-3 inhibits IL-12-induced STAT4 activation by binding through its SH2 domain to the STAT4 docking site in the IL-12 receptor β2 subunit. Biochem Biophys Res Commun 2003;310:1188–93.
31. Seki Y, Inoue H, Nagata N, et al. SOCS-3 regulates onset and maintenance of T(H)2-mediated allergic responses. Nat Med 2003;9:1047–54.
32. Stoiber D, Kovarik P, Cohney S, Johnston JA, Steinlein P, Decker T. Lipopolysaccharide induces in macrophages the synthesis of the suppressor of cytokine signaling 3 and suppresses signal transduction in response to the activating factor IFN-γ. J Immunol 1999;163:2640–7.
33. Jo D, Liu D, Yao S, Collins RD, Hawiger J. Intracellular protein therapy with SOCS3 inhibits inflammation and apoptosis. Nat Med 2005;11:892–8.
34. Li Y, Chu N, Rostami A, Zhang GX. Dendritic cells transduced with SOCS-3 exhibit a tolerogenic/DC2 phenotype that directs type 2 Th cell differentiation *in vitro* and *in vivo*. J Immunol 2006;177:1679–88.
35. Baetz A, Frey M, Heeg K, Dalpke AH. Suppressor of cytokine signaling (SOCS) proteins indirectly regulate toll-like receptor signaling in innate immune cells. J Biol Chem 2004;279:54708–15.
36. Presek P, Reinacher M, Eigenbrodt E. Pyruvate kinase type M2 is phosphorylated at tyrosine residues in cells transformed by Rous sarcoma virus. FEBS Lett 1988;242:194–8.